Solvation of a Probe Molecule by Fluid Supercooled Water in a Hydrogel at 200 K

Maria Grazia Santangelo,[†] Matteo Levantino,[‡] Antonio Cupane,[‡] and Gunnar Jeschke*[,†]

Laboratory of Physical Chemistry, ETH Zurich, Wolfgang-Pauli-Strasse 10, CH-8093 Zurich, Switzerland and Department of Physical and Astronomical Sciences (DSFA), University of Palermo, via Archirafi 36, I-90123 Palermo, Italy

Received: June 11, 2008; Revised Manuscript Received: October 2, 2008

By combining electron paramagnetic resonance (EPR) measurements on a nitroxide probe and differential scanning calorimetry (DSC), we demonstrate existence of liquid supercooled water in a silica hydrogel with high hydration level down to temperatures of at least 198 K. Besides the major fraction of liquid supercooled water, a minor fraction crystallizes at about 236 K during cooling and melts at 246 K during heating. The liquid domains are of sufficient size to solvate the nearly spherical paramagnetic probe molecule TEMPO with a diameter of about 6 Å. Analysis of EPR spectra provides the rotational correlation time of the probe that is further used to compare the viscosity of the supercooled water with the one of bulk water. In the temperature interval investigated, the supercooled water behaves as a fragile liquid and eventually solidifies at 120 K to a glass that incorporates the probe molecules.

Introduction

Water plays a fundamental and ubiquitous role in all aspects of life phenomena. Although water has been the topic of considerable research, its physical properties are not fully understood. Below the melting point at 273 K, it is possible to supercool bulk water down to ~235 K, where it crystallizes.[1] It is also possible to rapidly quench small quantities of water to temperatures below 100 K to form amorphous solid water, that is, glassy water. When heating glassy water, it exhibits a glass-liquid transition at a temperature, T_g, in the 124−136 K temperature interval[2,3] and then, because of the increased mobility of the molecules, it crystallizes at 150 K.[1] There is thus an experimentally inaccessible temperature region (so-called no man's land) for bulk supercooled water between roughly 150 and 235 K. The temperature dependence of the viscosity and relaxation time above this temperature region follows a power law that diverges at a critical temperature $T_s \approx 228$ K.[4]

Confined water is of importance because it provides a means of entering into the inaccessible temperature region for bulk supercooled water.[5,6] In given geometrical confinements, water molecules are unable to form a crystalline structure. Thus, water remains fluid and, like any other supercooled liquid, becomes increasingly viscous as the temperature approaches T_g. Geometric confinement is expected to induce modifications on both the structural and dynamic properties of bulk water. Studies on water in confined geometries are also of relevance for biological implications, since water confined at protein surfaces has been suggested to be important to protein stability and function.[7,8]

Sol−gel techniques for the preparation of silica hydrogels offer a new way of obtaining water confined in a three-dimensional disordered and hydrophilic matrix that provides an environment for water similar to the one near protein surfaces. Studies on water confined in silica hydrogels, using optical absorption spectroscopy in the near-infrared region (NIR), have provided information on the thermodynamic equilibrium between different classes of water molecules.[9] In particular, in a three-months aged "dry" hydrogel, a fraction (~5%) of weakly bonded water molecules is always present, even at 5 K. In contrast, in the case of a one-day aged "wet" hydrogel, crystallization of water occurs between 265 and 250 K, thus preventing investigation with optical spectroscopy at lower temperatures; moreover, saturation of the signal does not allow evaluating the fraction of water that crystallizes in wet hydrogel.

To characterize the structural and dynamic properties of water confined in silica hydrogels, in this work we have used electron paramagnetic resonance (EPR) and differential scanning calorimetry (DSC). Silica hydrogels have been prepared starting from a dilute solution of an EPR probe (TEMPO) in water. The EPR spectrum of nitroxide molecules such as TEMPO is highly sensitive to the mobility of the spin probes; thus, information about the local environment of the probes can be obtained. On the other hand, DSC measurements provide quantitative and qualitative information about physical and chemical changes that involve endothermic or exothermic processes such as glass transition, crystallization, and melting transitions. Here we report the EPR spectra and DSC scans of wet silica hydrogels having an hydration level, h, equal to 4.5 (h is defined as the mass of water present in the gel divided by the mass of nonaqueous material) and containing the nitroxide probe TEMPO. Solutions of TEMPO in pure water and in a glycerol/water mixture (80% glycerol/20% water, v/v) have also been prepared and investigated with EPR as reference samples.

Experimental Methods

Preparation of Silica Hydrogels for EPR Measurements. The nitroxide radical 2,2,6,6-tetramethylpiperidine-1-oxyl (TEMPO) and the alkoxide tetramethyl-orthosilicate (TMOS) were purchased from Aldrich and Merck, respectively, and were used without further purification. A solution containing 75% v/v TMOS, 21% H_2O (Millipore purified), and 4% 0.05 mM HCl was sonicated for ~20 min and diluted with an equal volume of a 400 μM solution of TEMPO in water. Approximately 15 mg of the resulting mixture were poured into an EPR capillary tube (I.D. $\approx$ 700 μm) and left to age for about

* To whom correspondence should be addressed. Phone: +41-44-632-5702; fax: +41 −44-632-1021; e-mail: gunnar.jeschke@phys.chem.ethz.ch.
[†] ETH Zurich.
[‡] University of Palermo.

10.1021/jp805131j CCC: $40.75
Published on Web 11/17/2008

one day until the sample had solidified macroscopically. The gel was then purged for several minutes with dry nitrogen until its hydration level had dropped to $h = 4.5$. The final mass of water in this sample was about 10 mg. Measurements on samples with different hydration levels between $h = 4$ and $h = 5$, and the same aging time (~1 day), have also been performed and yielded essentially the same results. Thus, in the following, we will call "wet" all hydrogels having a hydration level $h = 4.5 \pm 0.5$ and an aging time of ~1 day.

A water sample and a glycerol/water mixture (80% glycerol/20% water, v/v) both containing 200 μM TEMPO were also prepared starting from a 2 mM stock solution of TEMPO in water and were poured into quartz EPR tubes having an I.D. of 500 μm and 2 mm, respectively. All aqueous solutions were prepared with Millipore ultrapure water. Reagent grade glycerol was purchased from ABCR GmbH and Co. KG.

Preparation of Silica Hydrogels for DSC Measurements. Wet hydrogels used for DSC measurements have been prepared following the same procedure used for EPR experiments but with two different sample geometries. In one case, after mixing the reagents as described previously, the resulting liquid was poured into a standard stainless steel pan for DSC measurements. Because of the large surface-to-volume ratio, the water evaporation rate is much higher than in the case of the sample prepared in a capillary tube. After a few minutes from preparation, a hydration level $h = 4.4$ was reached; the DSC pan was then immediately sealed and left to age for about one day before performing the DSC measurements. This sample contained about 34 mg of water. To be able to more directly compare the EPR and DSC experiments, DSC scans were also performed on a wet hydrogel prepared into a capillary tube identical to that used for EPR measurements. In particular, after pouring the sample into the capillary tube, it was left to age for about one day until it had solidified macroscopically. The sample was then purged for several minutes with dry nitrogen until its hydration level had dropped to $h = 4.1$. At this point, the bottom part (about 5 mm) of the capillary tube containing the silica hydrogel was cut, put inside a DSC stainless steel pan, and sealed. The DSC measurements were performed right after sealing the pan. The final mass of water in this sample was about 1.6 mg.

EPR Spectroscopy. Continuous-wave (cw) EPR measurements at X-band were carried out using a Bruker ELEXSYS E500 spectrometer equipped with a Bruker superhigh-Q ER-4122SHQ cavity. Cooling of the sample was performed with a liquid nitrogen dewar vessel and a Bruker ER-4111VT temperature control unit. Measurement parameters were as follows: microwave frequency $\approx$ 9.5 GHz and modulation frequency = 100 kHz. To avoid signal distortion due to excessive magnetic field modulation, at each temperature, the modulation amplitude was chosen to be about one-third of the EPR linewidth. A saturation study on the samples allowed us to ensure that, at each temperature, the microwave power incident on the sample did not induce saturation.

DSC Characterization. Measurements were performed with a PerkinElmer PYRIS Diamond differential scanning calorimeter equipped with a liquid nitrogen cooling system that allows operation down to about 95 K. Both the temperature and heat-flow scale of the DSC instrument were calibrated using a high purity indium reference sample. Measurements have been performed on samples sealed inside standard DSC stainless steel pans against an empty pan placed in the reference vessel of the instrument. The temperature was lowered from ambient to 95 K at 10 K/min, held at 95 K for 5 min, and then raised at 10 K/min toward room temperature while monitoring for any exothermic or endothermic process. Scans at 3 K/min were also performed. The small differences in transition temperatures between the faster and the slower scans do not affect interpretation of the data.

The crystallization and melting temperatures of water encapsulated in our wet hydrogels were directly determined from the DSC scans. The fraction of water molecules that crystallizes/melts in wet hydrogels was obtained by dividing the area of the crystallization/melting peaks by the water latent heat of melting, assuming that water encapsulated in our silica gels is characterized by a latent heat for melting very close to that of bulk water.

Theory and EPR Data Analysis. The lineshapes of the cw EPR spectra of nitroxide probes at X-band frequencies are dominated by the hyperfine coupling of the unpaired electron of the N−O group to the ^{14}N nucleus with nuclear spin $I = 1$. For a molecule at a given orientation this hyperfine coupling causes a splitting of the EPR line into three lines corresponding to magnetic quantum numbers $m_I = -1$, 0, and 1 of the ^{14}N nucleus. The magnitude of this splitting depends on orientation, as the unpaired electron is localized in a $2p_z\pi$-orbital whose lobes define the z-direction of the molecular frame. Along this z-direction, the hyperfine coupling (A_{zz}) is maximum, whereas it is minimum in the plane perpendicular to it ($A_{xx} \approx A_{yy}$).

The temperature dependence of EPR spectra of nitroxide probes is due to changes of the probe's motion that can be characterized by its rotational correlation time, τ_c. If the probe rotates with a rate that exceeds the magnitude of the anisotropy of the hyperfine interaction (fast motion regime), the resulting spectrum shows a simple triplet pattern characterized either by uniform (average or isotropic spectra, $\tau_c \lesssim 10$ ps) or nonuniform linewidths (10 ps $\lesssim \tau_c \lesssim 4$ ns). For correlation times $\tau_c \gtrsim 4$ ns, dynamics is slow on the EPR time scale (slow motion regime), and the spectral lineshape becomes more complicated. Finally, if the probe molecules rotates with a rate that is smaller than the intrinsic linewidth ($\tau_c \gtrsim 1$ μs), a powder pattern results that is almost insensitive to changes in τ_c (rigid limit spectra). The slow down of the rotational correlation time τ_c as the temperature is lowered (or the viscosity increased) can be tracked by monitoring the separation, $2A'_{zz}$, between the outer lines of the nitroxide EPR spectrum. In the rigid limit $2A'_{zz}$ corresponds to twice the hyperfine coupling along the z-direction ($2A_{zz}$); in the fast limit, $2A'_{zz}$ approaches $2A_{iso}$, that is, twice the isotropic hyperfine coupling (A_{iso}).

Apart from the sensitivity of the EPR technique to the spin probe motion, the different EPR parameters associated with a spin probe show a solvent dependence. In particular, the hyperfine coupling component perpendicular to the plane of the ring structure of TEMPO, A_{zz}, the isotropic hyperfine coupling, A_{iso},[10] and the g_x element of the g-tensor,[11] are sensitive to the polarity of the local environment.[12,13] Thus, by comparing the EPR parameters obtained for TEMPO in wet hydrogel and in bulk water, it is possible to get information about the relative polarity of our samples. Since with the X-band spectra we could not have accurate estimates of the g_x and A_{zz} parameters, we restrict ourselves to comparing A_{iso} parameters to obtain information about the polarity of our samples.

A general theory that relates τ_c to the spectral width of the EPR lines has been derived in the past by Kivelson.[14] In the case of nitroxide probes in fast motion, the equations derived by Kivelson can be combined to obtain the following expression:

$$\tau_c = \frac{\pi\sqrt{3}}{b}\left[\frac{b}{8} - \frac{4\Delta\gamma B_0}{15}\right]^{-1}\Delta\nu_0\left[\frac{\Delta\nu_{-1}}{\Delta\nu_0} - 1\right] \qquad (1)$$

where b is a constant that depends on the anisotropic hyperfine couplings, $\Delta\gamma$ is a constant that depends on the anisotropic g values, B_0 is the laboratory magnetic field, and $\Delta\nu_0$ and $\Delta\nu_{-1}$ are the peak-to-peak widths (in Hz) corresponding to the mid- and high-field lines, respectively. For convenience of measurement, the ratio $\Delta\nu_{-1}/\Delta\nu_0$ can be replaced by $(h_0/h_{-1})^{1/2}$, where h_0 and h_{-1} are the heights of the mid- and high-field lines of the first-derivative absorption spectrum; $\Delta\nu_0$ can be converted to the magnetic field peak-to-peak width, W_0. The resulting expression for the correlation time is:

$$\tau_c = kW_0\left[\sqrt{\frac{h_0}{h_{-1}}} - 1\right] \quad (2)$$

(see Supporting Information for details on the calculations of the constant k in our experimental conditions). This formula assumes an isotropic rotational diffusion tensor, characterized by the correlation time τ_c. This is appropriate for the almost spherical probe TEMPO, as long as specific interactions, such as hydrogen bonding to the N−O group, are negligible. Starting from the theory developed by Kivelson, it is possible to derive two alternative equations for τ_c, which depend also on the intensity, h_{+1}, of the low-field line. In particular:

$$\tau_c = \frac{\pi\sqrt{3}}{b}\left[\frac{4\Delta\gamma B_0}{15}\right]^{-1}\frac{g_0\mu_B}{h}W_0\frac{1}{2}\left[\sqrt{\frac{h_0}{h_{+1}}} - \sqrt{\frac{h_0}{h_{-1}}}\right] \quad (3)$$

$$\tau_c = \frac{\pi\sqrt{3}}{b}\left[\frac{b}{8}\right]^{-1}\frac{g_0\mu_B}{h}W_0\frac{1}{2}\left[\sqrt{\frac{h_0}{h_{+1}}} + \sqrt{\frac{h_0}{h_{-1}}} - 2\right] \quad (4)$$

If the hypothesis of isotropic rotation is correct, eqs 1, 3, and 4 should all give the same rotational correlation time (within experimental errors). In the case of TEMPO in wet silica hydrogel at 293 K, we obtain $\tau_c = 6.9 \times 10^{-11}$ s using eq 1, and 5.2×10^{-11} s and 8.6×10^{-11} s using eqs 3 and 4, respectively. The deviations between the three values are small on the logarithmic scale used for discussing temperature dependence. Moreover, good agreement has been obtained for all the temperatures in the fast motion regime and for all the samples investigated. This indicates that the rotational motion of the probe molecules is similar in bulk and in confined water and can be characterized to a good approximation by an isotropic rotational diffusion tensor.

A further assumption of eq 1 is that the intrinsic lineshapes of the spin probe EPR spectrum are Lorentzian. In fact, due to the presence of unresolved proton hyperfine structure, an inhomogeneous (typically Gaussian) broadening is also present.[15] To further test the validity of the isotropic hypothesis and to investigate the effect of a Gaussian broadening on the correlation time calculations, we have simulated the experimental spectra using the EasySpin[16] function "chili", which is based on the stochastic Liouville equation (SLE). The simulations assumed an isotropic rotational diffusion tensor. Moreover, in order to reproduce the experimental lineshapes, both a Gaussian and a Lorentzian contribution to the total linewidth had to be assumed. The agreement between the simulations and the experimental data was good for all three different samples investigated (TEMPO in wet hydrogel, in water, and in 80% glycerol/H_2O mixture), and the τ_c values obtained from the simulations were very similar to the τ_c values obtained using eq 1 (see Supporting Information for some examples of simulations of TEMPO in wet silica hydrogel). The similarity of the τ_c values between SLE fits and the Kivelson formula prove that, despite the inhomogeneous Gaussian broadening in our experimental spectra, the Kivelson formula is adequate for calculating rotational correlation times.

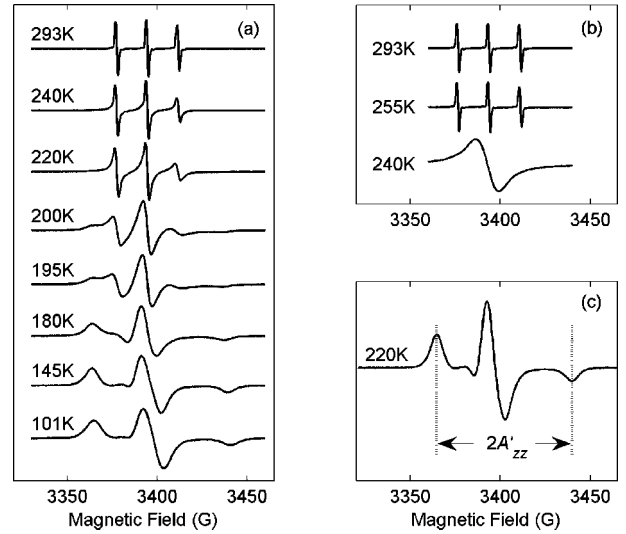

Figure 1. X-band EPR spectra of TEMPO in (a) a wet hydrogel (having a hydration level $h = 4.5$), (b) bulk water, (c) a glycerol/water mixture (80% glycerol/20% water, v/v) at different temperatures. The extreme outer peak separation, $2A'_{zz}$, is indicated in panel c in the case of TEMPO in 80% glycerol/H_2O at 220 K.

In the slow motion regime, we have estimated τ_c by using the correlation between A'_{zz} and τ_c. Assuming isotropic Brownian diffusion motion, spectra for 121 different values of τ_c between 10^{-11} and 10^{-5} s were simulated using software from the Freed group[17] and a spline interpolation of the A'_{zz} values was performed. Experimental A'_{zz} values were converted to correlation times τ_c by inverting the functional dependence $A'_{zz}(\tau_c)$ defined by the interpolating splines.

In the case of spherical molecules of radius r dissolved in an isotropic solvent at temperature T, the rotational correlation time is related to the solvent viscosity η through the Debye−Stokes−Einstein equation:

$$\tau_c = \frac{4\pi\eta r^3}{3k_BT} \quad (5)$$

where k_B is the Boltzmann constant. Since the specific interactions of the probe molecule with the solvent influence the dynamics of the probe,[18] eq 5 cannot be used to obtain accurate values of the macroscopic solvent viscosity. However, eq 5 can still be used to evaluate the relative viscosity of water confined in wet hydrogels with respect to that of bulk water or an 80% glycerol/H_2O mixture by comparing the temperature dependence of the rotational correlation times.

Results and Discussion

The cw EPR spectra at different temperatures of TEMPO in wet hydrogel, water, and 80% glycerol/H_2O are shown in Figure 1, panels a, b, and c, respectively. The spectra of TEMPO in wet hydrogel (Figure 1a) between room temperature and about 198 K are typical of nitroxides in the fast motion regime. This proves that the macroscopically solid sample contains water that can be supercooled at least down to 198 K (−75 °C). Decreasing the temperature, the dynamics of TEMPO molecules becomes

slower, and the spectra between 195 and 101 K are typical of probe molecules in a rigid environment.

When TEMPO is dissolved in pure water (Figure 1b) fast motion regime spectra are observed down to 255 K; at lower temperatures (between 255 and 240 K) water freezes and the TEMPO molecules tend to precipitate out of the crystalline lattice formed by water molecules. The cw EPR spectrum is now characterized by one broad peak due to exchange and dipolar interactions between the aggregated TEMPO molecules. Such behavior (well-known for solutions of TEMPO in bulk water) is not observed for TEMPO encapsulated in our wet hydrogel: the TEMPO molecules do not precipitate as they do in pure water. Nevertheless, from just the EPR data, we cannot exclude the formation of ice in wet hydrogels. We could either have a mixture of ice and liquid water, with the spin probes in the liquid fraction, or we might have a measurable fraction of the spin probes as impurities (defects) in the ice crystal, that is, a deformed ice lattice around the probe. The second hypothesis is less probable because, if an ice crystal forms inside a pore, it is reasonable to suppose that TEMPO molecules would tend to precipitate out of the crystalline phase, as is observed in the case of bulk water. Moreover, the shape of the cw EPR spectra above 200 K shows no evidence of TEMPO molecules in a rigid (ice-like) environment. Hence, we can conclude that TEMPO molecules are solvated in liquid water. The results further indicate that water molecules around TEMPO form a three-dimensionally continuous liquid phase. Indeed, in the case of the formation of a two-dimensional film around TEMPO we would expect specific directional interactions of the spin probes with the silica matrix resulting in an increase of the rotational diffusion anisotropy and a marked slowdown of the rotational diffusion time, which we do not observe.

Another feature of the wet silica hydrogel is revealed by comparing its cw EPR spectrum at a given temperature (Figure 1a) with the spectra, at the same temperature, of TEMPO in 80% glycerol/H_2O (Figure 1c) and in water solution (Figure 1b). At 220 K, while TEMPO molecules in the hydrogel are still in the fast motion regime, the TEMPO molecules in 80% glycerol/H_2O are already close to the rigid limit; this means that the viscosity of water within wet silica hydrogels is lower than that of an 80% glycerol/H_2O mixture at the same temperature. Conversely, at 293 K, the spectrum of TEMPO molecules in water solution corresponds to motion faster than in the hydrogel; this means that the viscosity of water within wet silica hydrogels is higher than that of a water solution at the same temperature.

A simple method for characterizing the nitroxide probe dynamics is to plot the extreme separation of the EPR outer lines ($2A'_{zz}$ parameter) as a function of temperature (Figure 2). In our wet hydrogel, the behavior of $2A'_{zz}$ is similar to that observed in a large number of synthetic polymers and low-molecular weight glass-formers.[19−21] Usually a characteristic temperature T_{50G} is identified, which corresponds to the temperature at which $2A'_{zz} = 50$ Gauss. If the probe size matches a characteristic length of the glass-forming matrix, the temperature T_{50G} corresponds to a "high frequency" glass transition temperature since it corresponds to the temperature at which the relaxation time crosses the window of $\sim 10^{-8}$ s; such a temperature is generally expected to be higher than, but correlated with, T_g (the calorimetric glass transition temperature). For probes that are much smaller than the molecules of the glass-forming matrix, T_{50G} may be lower than T_g. In the case at hand, the probe has a diameter of ~6 Å larger than that of a water molecule, so that the first case applies. From Figure 2, it is

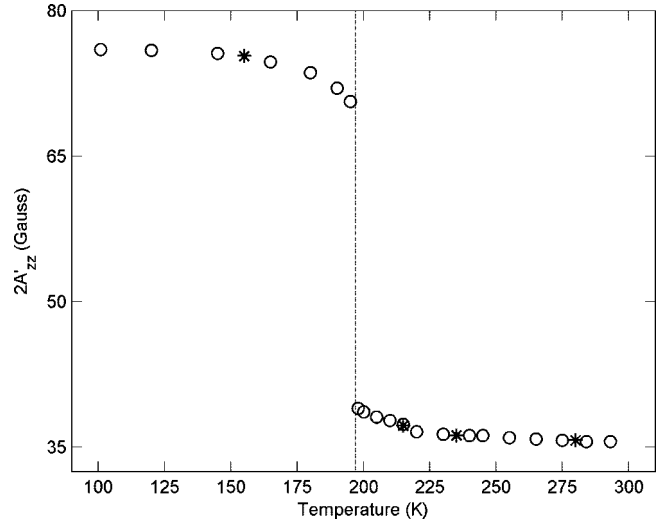

Figure 2. Temperature dependence of the outer peak separation ($2A'_{zz}$) characterizing the EPR spectra of TEMPO in a wet hydrogel (having a hydration level $h = 4.5$); data acquired on both lowering the temperature (circles) and raising the temperature (asterisks) are reported. The dashed line is a reference at 197 K.

observed that $2A'_{zz}$ undergoes a sharp transition between 200 and 195 K. We find $T_{50G} = 197$ K, indicating that water encapsulated in silica hydrogels can be supercooled at least down to about 198 K. Although the EPR experiments have been carried out cooling the sample from room temperature to 101 K, spectra at several selected temperatures have been recorded during a heating cycle after the sample had been brought down to 101 K. These data points (shown as asterisks in Figure 2) do not deviate significantly from the dependence observed during cooling, which suggests that no hysteresis is present. Further experiments showed that T_{50G} is the same during the heating and the cooling cycle (data not shown) thus excluding the presence of hysteresis. In contrast, for TEMPO in bulk water, although we were able to supercool the sample below its freezing point (down to 255 K), evidence of a liquid phase on heating was observed only when the sample was brought back above the water melting point (~273 K).

In the fast motion regime, $2A'_{zz}$ approaches $2A_{iso}$. In the case of TEMPO in silica hydrogel, we obtained $A_{iso} = 49.9$ MHz, whereas in the case of TEMPO in water $A_{iso} = 50.3$ MHz. The difference of the two values does not exceed experimental error. This is an indication that the polarity of the local TEMPO environment is similar in bulk water and in wet hydrogel, and it thus confirms that the probe in wet hydrogel, at least at room temperature, is solvated by water.

Figure 3 shows plots of the correlation time τ_c for TEMPO molecules in wet hydrogel and in 80% glycerol/H_2O as a function of the inverse temperature; the behavior of TEMPO in water solution is also reported for comparison. For all samples, τ_c values increase by decreasing the temperature; a saturating behavior is observed at temperatures well below T_{50G}, where free rotational motion no longer occur on the EPR time scale and the spectral lineshapes may be dominated by librational motion[22] or reorganization of the solvent cage.[23] The values of τ_c obtained by fitting lineshapes with a model of isotropic rotational diffusion thus do not have a clear physical interpretation at temperatures well below T_{50G}. Although in the whole temperature range the correlation times of both samples have a similar behavior, we could observe that the dynamics of TEMPO molecules in silica hydrogels is always faster than that of TEMPO in a 80% glycerol/H_2O mixture; moreover, in the

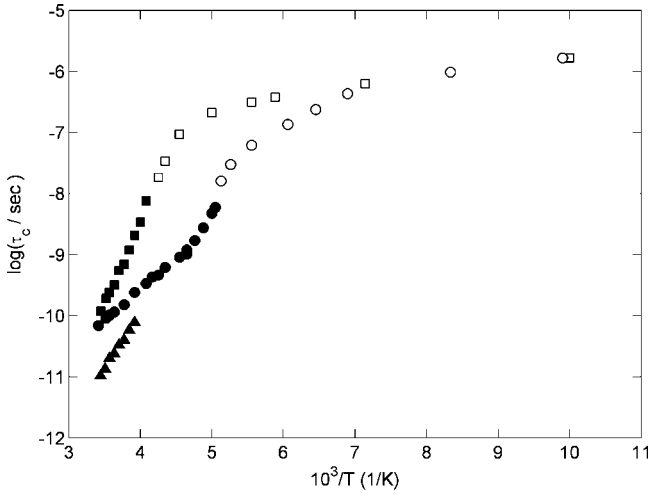

Figure 3. Temperature dependence of the rotational correlation time (τ_c) of TEMPO in wet hydrogel (circles), in a glycerol/water mixture (80% glycerol/20% water, v/v) (squares) and in bulk water (triangles). The filled symbols correspond to the fast motion regime, the open symbols correspond to the slow motion regime.

TABLE 1: Values of the Arrhenius and VFT Parameters Obtained by Fitting the Data in the Fast Motion Regime

	Arrhenius fitting		VFT fitting		
sample	log (τ_0/s)	ΔH (kJ/mol)	log (τ_0/s)	D	T_0 (K)
TEMPO in wet silica hydrogel	−14	20	−12.14	10.13	91.5
TEMPO in 80% glycerol/H_2O	−19	52	−13.85	9.21	143.7

temperature interval of 290−255 K, the dynamics of TEMPO molecules in silica hydrogels is always slower than that of TEMPO in water solution. We may thus conclude that water confined in wet hydrogels is less viscous than an 80% glycerol/H_2O mixture but is more viscous than bulk water. The correlation times and viscosity of water confined in our wet silica hydrogels (having a hydration level $h = 4.5$) are larger than those for pure water (about a factor of 10 at 290 K), in agreement with results from dielectric relaxation spectroscopy and quasi-elastic neutron scattering on analogous silica hydrogels having a lower hydration level.[24,25]

The glass transition regime of supercooled fluids is characterized by a number of typical kinetic phenomena. On cooling, the correlation time can increase in a non-Arrhenius way by many orders of magnitude in a narrow temperature range. The deviation from thermally activated dynamics is called fragility, and typically the temperature dependence of the correlation time can be described using a Vogel−Fulcher−Tamman (VFT) law. To evaluate the fragility of water confined in wet silica hydrogels, we have tried to fit the data relative to the fast motion regime in terms of an Arrhenius law or a cooperative VFT law. Values of the parameters obtained by fitting in terms of the Arrhenius expression $\tau_c = \tau_0 \exp(\Delta H/RT)$ are shown in Table 1. A pre-exponential factor of 10^{-19} s, obtained for TEMPO in 80% glycerol/H_2O, appears quite unphysical; moreover, although a linear fit agrees reasonably well with both the experimental data sets in the rather limited temperature interval available, the extrapolations to low temperatures give values of T_{100s} (i.e., the temperature at which the correlation time reaches the value of 100 s, corresponding to the calorimetric glass transition) of 65 and 125 K for TEMPO in wet hydrogel and in 80% glycerol/H_2O, respectively, much lower than the calorimetrically measured values of 120 K (see below) and 180 K.[26] For the above reasons we performed fits in terms of the VFT expression $\tau_c = \tau_0 \exp[DT_0/(T - T_0)]$ imposing a τ_c of 100 s at the glass transition temperature; values of the VFT parameters are also shown in Table 1. Figure 4 reports an "Angell plot" of our experimental data;[27] the resulting VFT fits are reported as continuous lines and give excellent agreement with the experimental data indicating that both water confined in wet silica hydrogel and an 80% glycerol/H_2O mixture behave as fragile glass-formers.[28] The fragility parameter[27] m, defined as $m = d \log(\tau_c)/d(T_g/T)|_{T = Tg}$, can give a measure of the fragility and how large is the deviation from the Arrhenius law. From the extrapolation of the VFT behavior down to the glass transition temperature region, we have obtained a fragility parameter $m = 60$ for water in silica hydrogel and $m = 79$ for 80% glycerol/H_2O respectively. We note, however, that for water confined in wet silica hydrogel, we cannot exclude the onset of a fragile-to-strong transition[29,30] at temperatures lower than 200 K. Further experiments with techniques able to probe the dynamics of water in the time window from 100 ns to 100 s, such as dielectric spectroscopy,[31] are needed to clarify this point.

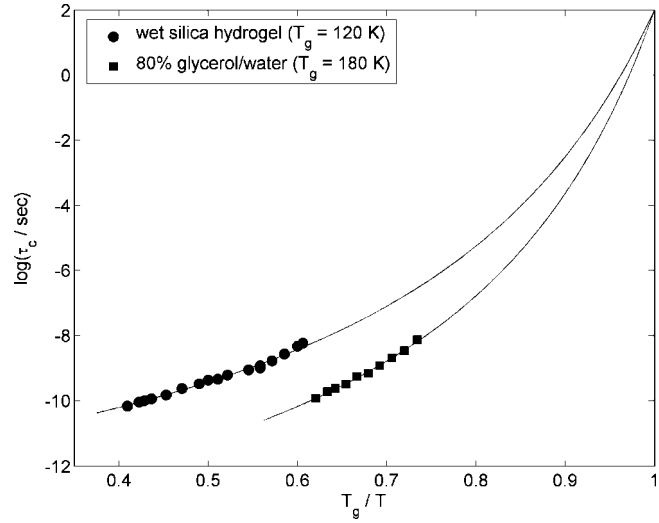

Figure 4. Angell plots for TEMPO in wet hydrogel (circles) and in a glycerol/water mixture (80% glycerol/20% water, v/v) (squares). The solid lines are best fits to a VFT law.

In Figure 5a we show the DSC scans of TEMPO in a wet hydrogel prepared directly into a steel pan. On cooling the sample, a crystallization peak is seen at about 240 K. This peak corresponds to the freezing of about 25% of the sample water content; the remaining water does not crystallize, at least down to 95 K. On heating the sample, a glass transition is observed at about 120 K (see left inset). A similar result has been recently obtained by the Oguni group using adiabatic calorimetry.[32] At higher temperatures, two melting peaks are seen: a small one at about 175 K and a large and broad one at about 255 K. The first melting peak (see right inset) is preceded by an exothermic peak at about 168 K, likely due to crystallization of a small fraction of supercooled water. The melting peak at 255 K is spread over a relatively large temperature interval. We interpret this spread as a result of the pore size distribution of the silica matrix; indeed, due to surface effects, the melting point depends on pore size.[33] Consistently, the amount of water that, on reheating, melts at about 255 K corresponds to the amount that had crystallized, on cooling, at about 240 K.

In Figure 5b we show the DSC scans of TEMPO in a wet hydrogel prepared into a capillary tube and then sealed inside a steel pan. The results are closely similar to the previous ones.

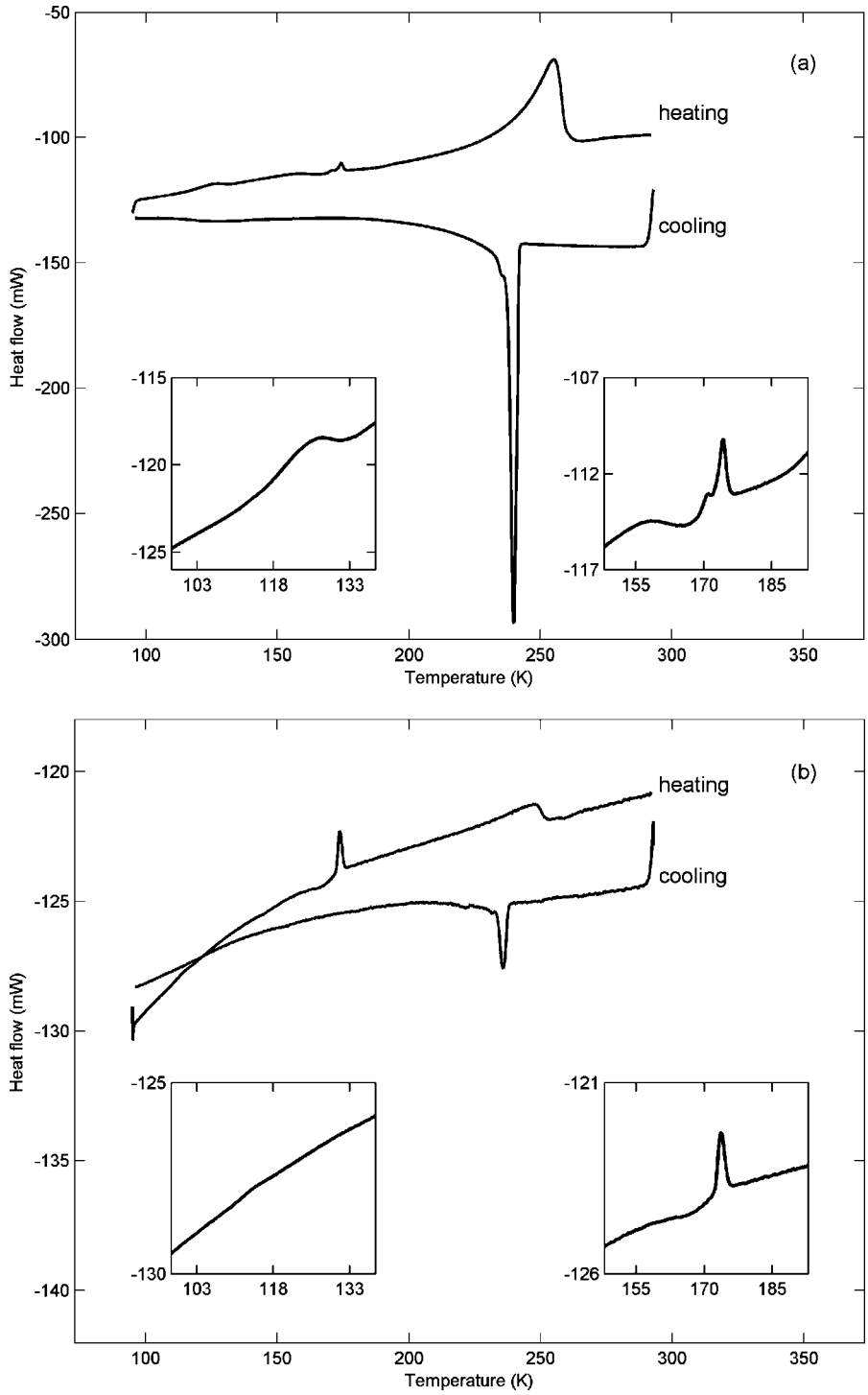

Figure 5. DSC scans of (a) a wet hydrogel ($h = 4.4$) containing TEMPO and prepared directly in a DSC steel pan, this sample contains 34 mg of water; (b) a wet hydrogel ($h = 4.1$) containing TEMPO and prepared inside a capillary tube that has been sealed inside a steel pan (see text for details); this sample contains 1.6 mg of water. Insets are magnified plots of regions in the heating cycle where glass transitions (left insets) or weak crystallization/melting peaks (right insets) are observed or expected.

On cooling the sample, a crystallization peak is seen at about 236 K, and it is due to the freezing of a fraction of water (about 9%). We note that the capillary tube facilitates supercooling of water inside our samples; indeed, it is possible to supercool a larger fraction of water (91% versus 75%) in the capillary tube sample with respect to that prepared in the DSC pan. The remaining water does not crystallize at least down to 95 K. On heating the sample, no glass transition is clearly detected. We attribute this failure to insufficient sensitivity for such a low amount of water; indeed, the capillary tube sample contains only 1.6 mg of water, as compared to 34 mg of the steel pan sample. A melting peak is observed at about 175 K, again preceded by a small crystallization peak at about 165 K (see right inset). A second much broader melting peak is observed at about 246 K. As in the steel pan sample, the amount of water that melts (at about 246 K) on reheating corresponds to the amount that had crystallized (at about 236 K) on cooling.

Combining the EPR results (Figure 2) and the DSC results (Figure 5) we could reach a characterization of the structural and dynamic properties of water confined in wet silica hydrogels.

From the DSC scans we have seen that all water encapsulated in our silica hydrogels remains liquid from room temperature down to 236 K. This is seen also from the cw EPR spectra (Figure 2) showing that, between room temperature and 236 K, TEMPO molecules are in the fast motion regime; water molecules around the probe are in liquid state. At about 236 K, only a minor fraction of the total mass of water contained in our sample freezes, whereas the large majority is still in a supercooled state at least down to 95 K. From the EPR data we see that TEMPO molecules below 236 K are still in the fast motion regime down to 198 K. This means that TEMPO molecules are solvated by the fraction of water that does not crystallize, confirming our previous hypothesis that the hydrogel contains both ice and supercooled water. Not surprisingly, the TEMPO molecules are excluded from the crystalline phase and are dissolved only in the liquid phase. Although from the DSC data we have evidence that the majority of water in our hydrogels does not crystallize at least down to 95 K, EPR data reveal that a sharp transition from the fast to the slow motion regime occurs at about 197 K (Figure 2). At temperatures slightly lower than 197 K, TEMPO molecules are immobilized with respect to the EPR time scale. Apparently, the rotational correlation time of TEMPO molecules with a diameter of 6 Å drops below 10^{-8} s at a temperature that is about 77 K higher than the DSC glass transition temperature of the solvent (120 K). The cw EPR spectra below about 190 K are typical of probe molecules in a rigid environment (Figure 1a) as evidenced by the sharp transition of the $2A'_{zz}$ parameter at approximately 197 K (Figure 2). The glass transition is hardly seen in the DSC scans of wet hydrogels prepared in capillary tubes (Figure 5b), although it is clearly observed instead in the DSC scans of the sample prepared directly into the steel pan (Figure 5a). Because the samples are practically the same (the only difference is the presence of the capillary tube), we assume that the glass transition takes place at the same temperature and is missed in the DSC scans of the smaller sample for lack of sensitivity. The solvated TEMPO molecules become mobile with respect to the EPR time scale at temperatures higher than about 200 K without any significant hysteresis between cooling and heating; on reheating at about 246 K all the water encapsulated in wet silica hydrogels is again in the liquid state.

Conclusions

Two different techniques, EPR and DSC, have been used to characterize the structural and dynamic properties of water confined in wet silica hydrogels. These macroscopically solid samples prepared through a sol−gel protocol have a hydration level much higher than most samples used for studies on the dynamics of water in confinement.[24,34,35] In our samples, TEMPO spin probes and water molecules are confined inside silica matrix pores. In a previous work, using optical absorption spectroscopy in the near-infrared region, we found water crystallization in wet hydrogels below 265 K. The new results reveal that, in fact, only a small fraction of water confined in our matrix freezes, and the rest is supercooled at least down to 95 K; at this temperature (lower than the glass transition temperature) the sample contains an heterogeneous mixture of ice and amorphous solid water. Probably, as the temperature is lowered below 236 K, ice nanocrystals form inside the pores but a substantial fraction (between 75% and 90%) of water remains liquid. Therefore, it is possible with such silica hydrogels to access the no man's land for bulk water, that is, the temperature region between roughly 150 and 235 K. It should thus be possible, using different spectroscopic techniques like broadband dielectric spectroscopy, NMR, FTIR, and quasielastic neutron scattering, to study the structural and dynamic properties of water in this region. The samples exhibit a glass transition at approximately 120 K. Furthermore, we observed that TEMPO molecules encapsulated in our silica hydrogels are always dissolved in the water liquid phase and are in the fast motion regime with respect to EPR time scales down to 198 K. TEMPO molecules do not phase separate, upon immobilization, from water in wet hydrogels, they rather remain solvated. This is in contrast to the behavior observed in pure water, but characteristic for a glass-former. The size of amorphous or liquid domains exceeds the probe size of 6 Å. Larger EPR probes could be used to obtain an upper limit for the characteristic domain size. A possible application of the above results is the encapsulation of metalloprotein water solutions in silica hydrogels; without using cryoprotectants (like glycerol), one could thus study the dynamics of metalloproteins by EPR spectroscopy below the crystallization temperature of water.

Acknowledgment. We thank I. Garcia Rubio and I. Gromov for many fruitful discussions and G. Bellavia for generous assistance with the DSC measurements. A special thank is for Professor Arthur Schweiger (deceased) for the great support given at the beginning of this work. We acknowledge a grant from the Italian MIUR (PRIN2005) for financial support.

Supporting Information Available: Details on the correlation time calculations and a discussion on the simulation approach. This material is available free of charge via the Internet at http://pubs.acs.org.

References and Notes

(1) Mishima, O.; Stanley, H. E. *Nature* **1998**, *396*, 329.
(2) Johari, G. P.; Hallbrucker, A.; Mayer, E. *Nature* **1987**, *330*, 552.
(3) Handa, Y. P.; Klug, D. D. *J. Phys. Chem.* **1988**, *92*, 3323.
(4) Speedy, R. J.; Angell, C. A. *J. Chem. Phys.* **1976**, *65*, 851.
(5) Bergman, R.; Swenson, J. *Nature* **2000**, *403*, 283.
(6) Faraone, A.; Liu, L.; Mou, C. Y.; Yen, C. W.; Chen, S. H. *J. Chem. Phys.* **2004**, *121*, 10843.
(7) Rupley, J. A.; Careri, G. *Adv. Protein Chem.* **1991**, *41*, 37.
(8) Santangelo, M. G.; Levantino, M.; Vitrano, E.; Cupane, A. *Biophys. Chem.* **2003**, *103*, 67.
(9) Cupane, A.; Levantino, M.; Santangelo, M. G. *J. Phys. Chem. B* **2002**, *106*, 11323.
(10) Griffith, O. H.; Dehlinger, P. J.; Van, S. P. *J. Membr. Biol.* **1974**, *15*, 159.
(11) Kawamura, T.; Matsunam, S; Yonezawa, T. *Bull. Chem. Soc. Jpn.* **1967**, *40*, 1111.
(12) Owenius, R.; Engstrom, M.; Lindgren, M.; Huber, M. *J. Phys. Chem. A* **2001**, *105*, 10967.
(13) Kurad, D.; Jeschke, G.; Marsh, D. *Biophys. J.* **2003**, *85*, 1025.
(14) Kivelson, D. *J. Chem. Phys.* **1960**, *33*, 1094.
(15) Marsh, D. *Biological Magnetic Resonance Spin Labeling: Theory and Applications*; Berliner, L. J., Reuben J. Eds.: Plenum Publishing Corporation: New York and London, 1989; Vol. 8.
(16) Stoll, S.; Schweiger, A. *J. Magn. Reson* **2006**, *178*, 42.
(17) Schneider, D. J.; Freed, J. H. *Biol. Magn. Reson* **1989**, *8*, 1.
(18) Zager, S. A.; Freed, J. H. *J. Chem. Phys.* **1982**, *77*, 3344.
(19) Cameron, G. G. *Comprehensive Polymer Science: The Synthesis, Characterization, Reactions and Applications of Polymers*; Pergamon: Oxford, 1989; Vol. 1.
(20) Veksli, Z.; Andreis, M.; Rakvin, B. *Prog. Polym. Sci.* **2000**, *25*, 949.
(21) Švajdlenková, H.; Račko, D.; Bartoš, J. *J. Non-Cryst. Solids* **2008**, *354*, 1855.
(22) Dzuba, S. A. *Spectrochim. Acta* **2000**, *56A*, 227.
(23) Kirilina, E. P.; Grigoriev, I. A.; Dzuba, S. A. *J. Chem. Phys.* **2004**, *121*, 12465.
(24) Cammarata, M.; Levantino, M.; Cupane, A.; Longo, A.; Martorana, A.; Bruni, F. *Eur. Phys. J. E* **2003**, *12*, S63.
(25) Schirò, G.; Sclafani, M.; Caronna, C.; Natali, F.; Plazanet, M.; Cupane, A. *Chem. Phys.* **2008**, *345*, 259.

(26) Chen, B.; Sigmund, E. E.; Halperin, W. P. *Phys. Rev. Lett.* **2006**, *96*, 145502.
(27) Bohmer, R.; Ngai, K. L.; Angell, C. A.; Plazek, D. J. *J. Chem. Phys.* **1993**, *99*, 4201.
(28) Cook, R. L.; King, H. E.; Herbst, C. A.; Herschbach, D. R. *J. Chem. Phys.* **1994**, *100*, 5178.
(29) Ito, K.; Moynihan, C. T.; Angell, C. A. *Nature* **1999**, *398*, 492.
(30) Mallamace, F.; Broccio, M.; Corsaro, C.; Faraone, A.; Wanderlingh, U.; Liu, L.; Mou, C. Y.; Chen, S. H. *J. Chem. Phys.* **2006**, 124, 161102.
(31) Capaccioli, S.; Ngai, K. L.; Shinyashiki, N. *J. Phys. Chem. B* **2007**, *111*, 8197.
(32) Oguni, M.; Maruyama, S.; Wakabayashi, K.; Nagoe, A. *Chem. Asian J.* **2007**, *2*, 514.
(33) Alcoutlabi, M.; McKenna, G. B. *J.Phys.: Condens. Matter* **2005**, *17*, R461.
(34) Chen, S. H.; Mallamace, F.; Mou, C. Y.; Broccio, M.; Corsaro, C.; Faraone, A.; Liu, L. *Proc. Natl. Acad. Sci. U.S.A* **2006**, *103*, 12974.
(35) Bruni, F.; Ricci, M. A.; Soper, A. K. *J. Chem. Phys.* **1998**, *109*, 1478.

JP805131J